A novel fast mechanism for GPCR-mediated signal transduction—control of neurotransmitter release

Yonatan M. Kupchik,[1] Ofra Barchad-Avitzur,[1] Jürgen Wess,[2] Yair Ben-Chaim,[1] Itzchak Parnas,[1] and Hanna Parnas[1]

[1]Department of Neurobiology, Institute of Life Sciences, The Edmond Safra campus, The Hebrew University, Jerusalem 91904, Israel
[2]Molecular Signalling Section and Molecular Recognition Section, Laboratory of Bioorganic Chemistry, National Institute of Diabetes and Digestive and Kidney Diseases, National Institutes of Health, Bethesda, MD 20892

Reliable neuronal communication depends on accurate temporal correlation between the action potential and neurotransmitter release. Although a requirement for Ca^{2+} in neurotransmitter release is amply documented, recent studies have shown that voltage-sensitive G protein–coupled receptors (GPCRs) are also involved in this process. However, how slow-acting GPCRs control fast neurotransmitter release is an unsolved question. Here we examine whether the recently discovered fast depolarization-induced charge movement in the M_2-muscarinic receptor (M_2R) is responsible for M_2R-mediated control of acetylcholine release. We show that inhibition of the M_2R charge movement in *Xenopus* oocytes correlated well with inhibition of acetylcholine release at the mouse neuromuscular junction. Our results suggest that, in addition to Ca^{2+} influx, charge movement in GPCRs is also necessary for release control.

Introduction

Communication between neurons depends primarily on rapid neurotransmitter release. For such communication to be reliable, the kinetics of neurotransmitter release must be robust and release should begin very shortly after the action potential.

The amply documented hypothesis for fulfilment of these requirements is that the action potential opens Ca^{2+} channels to allow rapid influx of Ca^{2+}. The entered Ca^{2+} finalizes exocytosis of the "release-ready" vesicles (Calakos and Scheller, 1996; Murthy and De Camilli, 2003; Sudhof, 2004). The evidence for the primacy of Ca^{2+} in regulating action potential (depolarization)–evoked neurotransmitter release is overwhelming (Neher and Sakaba, 2008). However, it was shown both for cholinergic (Slutsky et al., 2001, 2003) and glutamatergic (Kupchik et al., 2008) synapses that in addition to Ca^{2+}, G protein–coupled receptors (GPCRs) are also involved in release control.

The notion that the GPCRs may control depolarization-evoked release is supported by the following findings. Immunoprecipitation experiments in rat brain synaptosomes showed that the M_2R coprecipitates with key proteins of the release machinery (Linial et al., 1997). Also, it was shown that the M_2R controls the kinetics of acetylcholine (ACh) release (Slutsky et al., 2001, 2003), whereas a glutamatergic GPCR controls the kinetics of glutamate release (Kupchik et al., 2008). In wild-type (WT) mice (Datyner and Gage, 1980; Slutsky et al., 2003) and in other preparations (Andreu and Barrett, 1980; Hochner et al., 1991; Bollmann and Sakmann, 2005) the kinetics of depolarization-evoked release is insensitive to changes in the concentration and kinetics of presynaptic Ca^{2+}. In contrast, the kinetics of Ca^{2+} uncaging-induced release (without depolarization) is sensitive to changes in the concentration of Ca^{2+} (Schneggenburger and Neher, 2000; Felmy et al., 2003b; Bollmann and Sakmann, 2005). The kinetics of depolarization-evoked release does depend on Ca^{2+} influx and removal, but only in knockout mice lacking functional M_2R (M_2KO; Slutsky et al., 2003). ACh release in M_2KO mice differed from that in WT mice also in other aspects. Specifically, the rate of spontaneous release was

Y.M. Kupchik and O. Barchad-Avitzur contributed equally to this paper.

Correspondence to Hanna Parnas: hannap@huji.ac.il

Yair Ben-Chaim's present address is Department of Neuroscience, Johns Hopkins University School of Medicine, Baltimore, MD 21205.

Abbreviations used in this paper: ACh, acetylcholine; CCh, carbachol; CNB-carbachol, *N*-(α-carboxy-2nitrobenzyl) carbamylcholine; DI, dose inhibition; ENTC, excitatory nerve terminal current; EPSC, excitatory postsynaptic current; Gal, gallamine; GC, gating current; GIRK, G protein–activated inwardly rectifying K^+ current; GPCR, G protein–coupled receptor; IC_{50}, half maximal inhibitory concentration; M_2KO, M_2R knockout; M_2R, M_2-muscarinic receptor; Meth, methoctramine; mGluR, metabotropic glutamate receptor; NMJ, neuromuscular junction; TTX, tetrodotoxin; WT, wild type.

The Rockefeller University Press $30.00
J. Cell Biol. Vol. 192 No. 1 137–151
www.jcb.org/cgi/doi/10.1083/jcb.201007053

2.24-fold higher in M_2KO mice. Also, evoked release was higher in M_2KO mice but mainly at low depolarization. Furthermore, release in M_2KO mice started sooner and lasted longer than in WT mice (Slutsky et al., 2003).

Theoretical considerations (Khanin et al., 1997) led us to propose that control of release of a specific transmitter is achieved by the same presynaptic receptor that mediates feedback autoinhibition of release of that same transmitter. At least for the major neurotransmitters these receptors are GPCRs. Indeed, studying release of ACh (as a case study to test this hypothesis) we found that the M_2R that mediates autoinhibition of ACh release (Slutsky et al., 1999) also controls release of ACh (Slutsky et al., 2001, 2003). Evidence supporting this hypothesis was obtained also for glutamate release. In the crayfish neuromuscular junction (NMJ), a metabotropic glutamate receptor (mGluR) that is similar to group II mGluRs controls the kinetics of glutamate release, and GPCRs of this group exert feedback autoinhibition of glutamate release (Kew et al., 2001).

Feedback inhibition is slow, in the tens of seconds or even minutes range. In contrast, evoked release is fast, in the millisecond range; hence, different mechanisms must presumably underlie the two processes. To unravel the mechanism by which GPCRs may control transmitter release, we took control of release of ACh by the M_2R as a case study. Based on the results gathered from these studies (summarized in Parnas et al., 2000; Parnas and Parnas, 2007), the following scenario was suggested. At resting potential, proteins of the release machinery associate with the transmitter-bound high affinity GPCR (Linial et al., 1997; Ilouz et al., 1999), resulting in tonic block of release ("brake"; Slutsky et al., 1999). Upon depolarization, the GPCR shifts to a low affinity state (Ben-Chaim et al., 2003; Ohana et al., 2006), the transmitter dissociates, the unbound GPCR detaches from the release machinery (Linial et al., 1997), and the brake is alleviated. The free release machinery, together with Ca^{2+} that had already entered, initiates release. Thus, we assumed that two factors control release; Ca^{2+}, which is essential for the exocytosis itself, and another factor that relieves the brake imposed by the presynaptic GPCR on the release machinery. But, what this other factor is and how the brake is removed remained unknown.

Recently we found that, like voltage-gated channels, the M_2R displays depolarization-induced rapid charge movement-associated currents (denoted, as for channels, "gating currents" [GCs]. We will use GCs and charge movement interchangeably; Ben-Chaim et al., 2006). This finding offered, for the first time, a novel unexpected avenue to seek for the "other" factor necessary for release. Specifically, we examine the possibility that the action potential, in addition to opening Ca^{2+} channels, also induces GCs in a controlling GPCR, and that these GCs are involved in the removal of the brake from the release machinery and hence in release initiation.

Results

Carbachol inhibits GCs and reduces release to a similar extent

To check for a possible linkage between GCs in GPCRs and release of neurotransmitter we sought pharmacological means to reversibly modulate GCs. We took the cholinergic system as a case study. There, a prototypical GPCR, the M_2R, controls ACh release (Slutsky et al., 2001, 2003). To date, measuring GPCR GCs from nerve terminals is not yet possible. Some of the main problems are that nerve terminals contain ionic channels, some of which are voltage gated. Thus, the measurements will include mainly ionic currents. Even worse, the voltage-gated channels themselves display GCs that are much larger than those of the M_2R. Therefore, even with subtracting the ionic currents, the GCs of the channels are expected to mask those of the M_2R. Finally, an extra complication is that the GCs of the GPCR are extremely fast (Zohar et al., 2010), requiring a large bandwidth and fast time resolution that is not easily achievable in the preparations available. We therefore measured GCs in M_2R-expressing *Xenopus* oocytes. We found that the natural agonist of muscarinic receptors, ACh, inhibited the GCs (Fig. S1 A; water-injected oocytes did not exhibit GCs [Fig. S1 B]).

To study the putative effect of inhibition of GCs on ACh release we needed to apply the inhibiting agonist shortly before the depolarizing pulse to prevent long-term effects on release. To this end, we used flash photolysis of the only muscarinic agonist available in a caged form, *N*-(α-carboxy-2nitrobenzyl) carbamylcholine (CNB-carbachol). This enables elevation of the local concentration of carbachol ($[CCh^*]_{local}$) within microseconds (Milburn et al., 1989). Before examining the effect of flash photolysis of CNB-carbachol on release, we checked its effect on GCs in M_2R-expressing oocytes. We found that flash photolysis of CNB-carbachol 3 ms before the depolarizing pulse inhibited the GCs (Fig. 1 A; we use here and below "flash" to mean flash photolysis of CNB-carbachol). However, the yield of the flash when used in the oocyte setup was very low (<0.1%), hence ineffective for evaluating full dose-dependent curves. Being satisfied that the inhibition of the GCs by carbachol (CCh) is very fast, we could thus use steady-state application of CCh to measure the dose-dependent effect of CCh on the GCs. Fig. 1 B shows that steady-state CCh inhibited the GCs dose dependently. The normalized (to control) GC dose-inhibition (DI_{GCs}) curve showed an $IC_{50\text{-}GCs}$ (IC_{50} for the DI_{GCs}) of 1.34 ± 0.10 µM (Fig. 1 C, 40-ms pulse). The DI_{GCs} curve of a 1-ms depolarizing pulse, similar in duration to the axonal action potential, showed a similar $IC_{50\text{-}GCs}$ (1.52 ± 0.20 µM, Fig. 1 C; $P > 0.3$).

Measurement of neurotransmitter release was performed on the mouse diaphragm NMJ using the macropatch technique (Dudel, 1981; Slutsky et al., 2003). An action potential was produced by a focal brief (0.2 ms) depolarizing pulse and the excitatory postsynaptic currents (EPSCs) were recorded with the same electrode. When threshold was reached, an all-or-none jump in the amplitude of the EPSCs was seen (unpublished data). To study the putative effect of inhibition of GCs on ACh release, the flash was applied 1 ms before the depolarizing test pulse. In these experiments, $[CCh^*]_{local}$ was ∼4% of the $[CNB\text{-}carbachol]_o$ (Fig. S2). Flash photolysis of CNB-carbachol reduced the EPSC dose dependently (Fig. 1 D) without affecting the quantum size (Fig. 1 E). The reduction of release was mediated by the M_2R as flash photolysis was ineffective in M_2KO mice (Fig. 1 F) even at the highest $[CCh^*]_{local}$ used for the WT mice. A release dose-inhibition ($DI_{release}$) curve was constructed

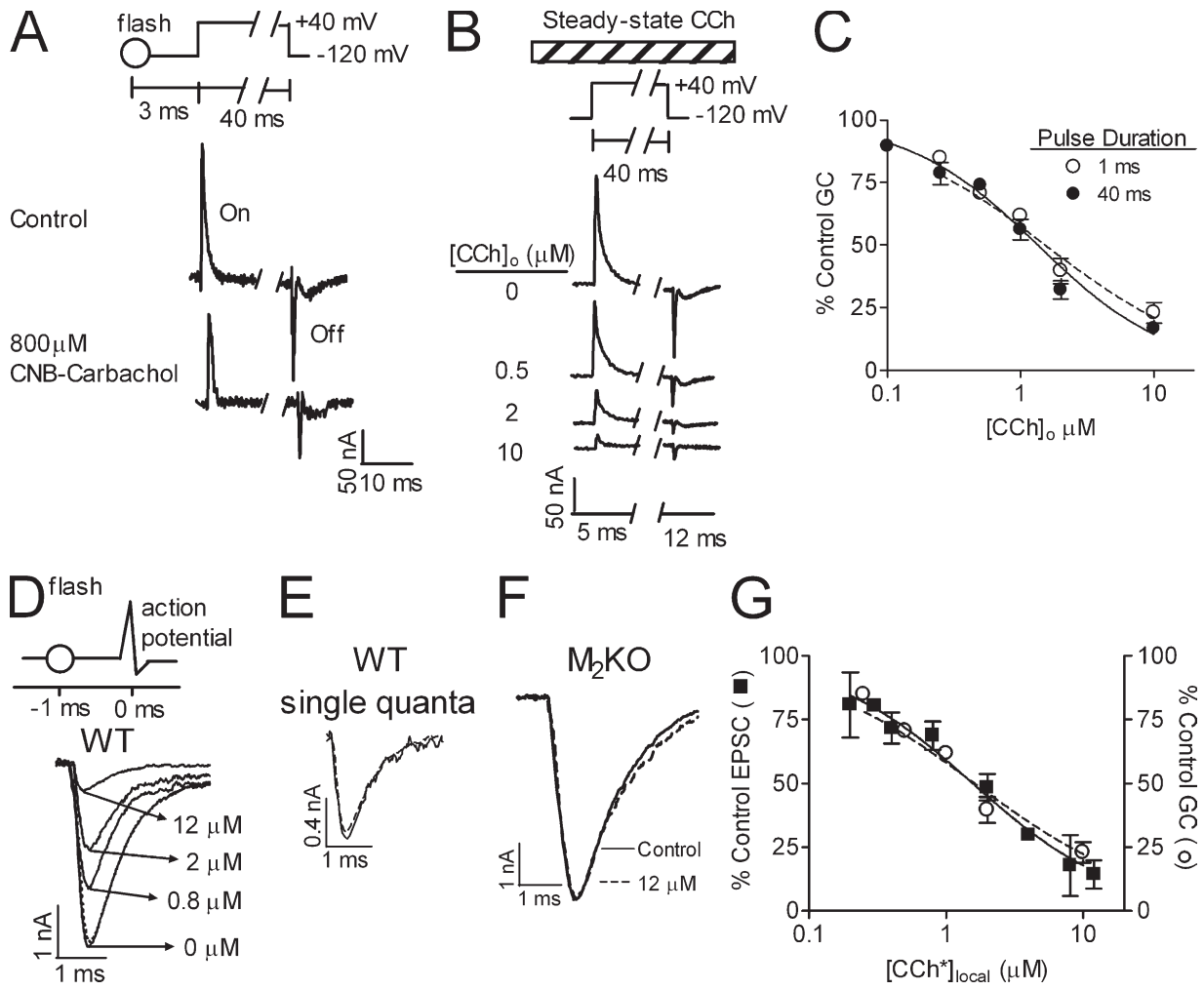

Figure 1. **Dependence of GCs and EPSCs on CCh.** (A) Representative samples (n = 8) of GCs measured in *Xenopus* oocytes before (top) and 3 ms after (bottom) flash photolysis of CNB-carbachol (800 μM). "On" = GCs produced during the depolarizing pulse. The flash inhibited the GCs to 61% of control. "Off" = GCs produced upon return to the holding potential. Inset shows the pulse protocol. (B) Samples of GCs at different steady-state $[CCh]_o$ measured in the same oocyte. Inset shows the pulse protocol. $[CCh]_o$ (bar) was present throughout the experiment. (C) Normalized DI_{GCs} curves for a depolarizing pulse of 40 (●) or 1 (○) ms with steady-state $[CCh]_o$. In each oocyte, GCs were measured in control and with one $[CCh]_o$ (n = 3–13 for each point taken from 14 donors). (D) EPSCs recorded in NMJs of WT mice in various $[CCh^*]_{local}$ as indicated. Inset shows pulse protocol. The flash (○) was given 1 ms before the action potential. (E) Single quanta (each trace average of 4 quanta) were recorded in control (solid line) and after a flash (dashed line) producing $[CCh^*]_{local}$ = 12 μM. (F) EPSCs evoked in M_2KO mice before (solid line) and 1 ms after the flash (dashed line) producing 12 μM $[CCh^*]_{local}$. (G) Data as in D presented as percentage of control EPSC (■, n = 4). "○" represents the 1-ms DI_{GCs} curve from B. For all figures, data points represent mean ± SEM.

from data as those seen in Fig. 1 D (Fig. 1 G, $IC_{50\text{-release}}$ = 1.56 ± 0.19 μM). Comparing the $DI_{release}$ curve to the DI_{GCs} curve obtained in the oocytes with the 1-ms depolarizing pulse (Fig. 1 G) shows a good correlation between the two, suggesting, but not proving, a causal relationship between GCs and release.

$[CCh^*]_{local}$ does not alter depolarization-induced Ca^{2+} currents

GPCRs mediate voltage-dependent inhibition of Ca^{2+} channels (Dolphin, 1998). Thus, the flash of CCh could have affected release by decreasing Ca^{2+} influx. We therefore examined whether $[CCh^*]_{local}$ inhibited depolarization-induced Ca^{2+} currents. In these experiments an action potential was generated in the nerve bundle by a suction electrode, the excitatory nerve terminal current (ENTC) was recorded extracellularly, by the macropatch electrode, at the nerve terminal, and the Ca^{2+} current was evaluated from the ENTC (Fig. 2, A_1–A_4; Brigant and Mallart, 1982; Dudel, 1990). We first checked the sensitivity of the technique used to evaluate the Ca^{2+} currents. To do so, we decreased the size of the action potential by adding 50 nM TTX. As expected, both the ENTC and the EPSC were reduced (Fig. 2 B), and so was the amplitude of the Ca^{2+} current (Fig. 2 C). These results indicate that the technique used is sufficiently sensitive to detect changes in Ca^{2+} currents had they occurred.

We used the reduced-in-amplitude action potential to check whether the flash affects Ca^{2+} currents. Fig. 2 D shows that flash-induced elevation of $[CCh^*]_{local}$ to 12 μM (the highest concentration used here) reduced the EPSC to 19% of control. Yet, it did not affect the Ca^{2+} currents (Fig. 2 E). To further test the sensitivity of the technique, we measured the effect of elevated $[Mg^{2+}]_o$ (5 mM) on Ca^{2+} currents and on release. In these experiments the results of Fig. 2, D and E, where a flash was applied, served as control. In contrast to the lack of effect of the flash on Ca^{2+} currents, elevation of $[Mg^{2+}]_o$ decreased the Ca^{2+}

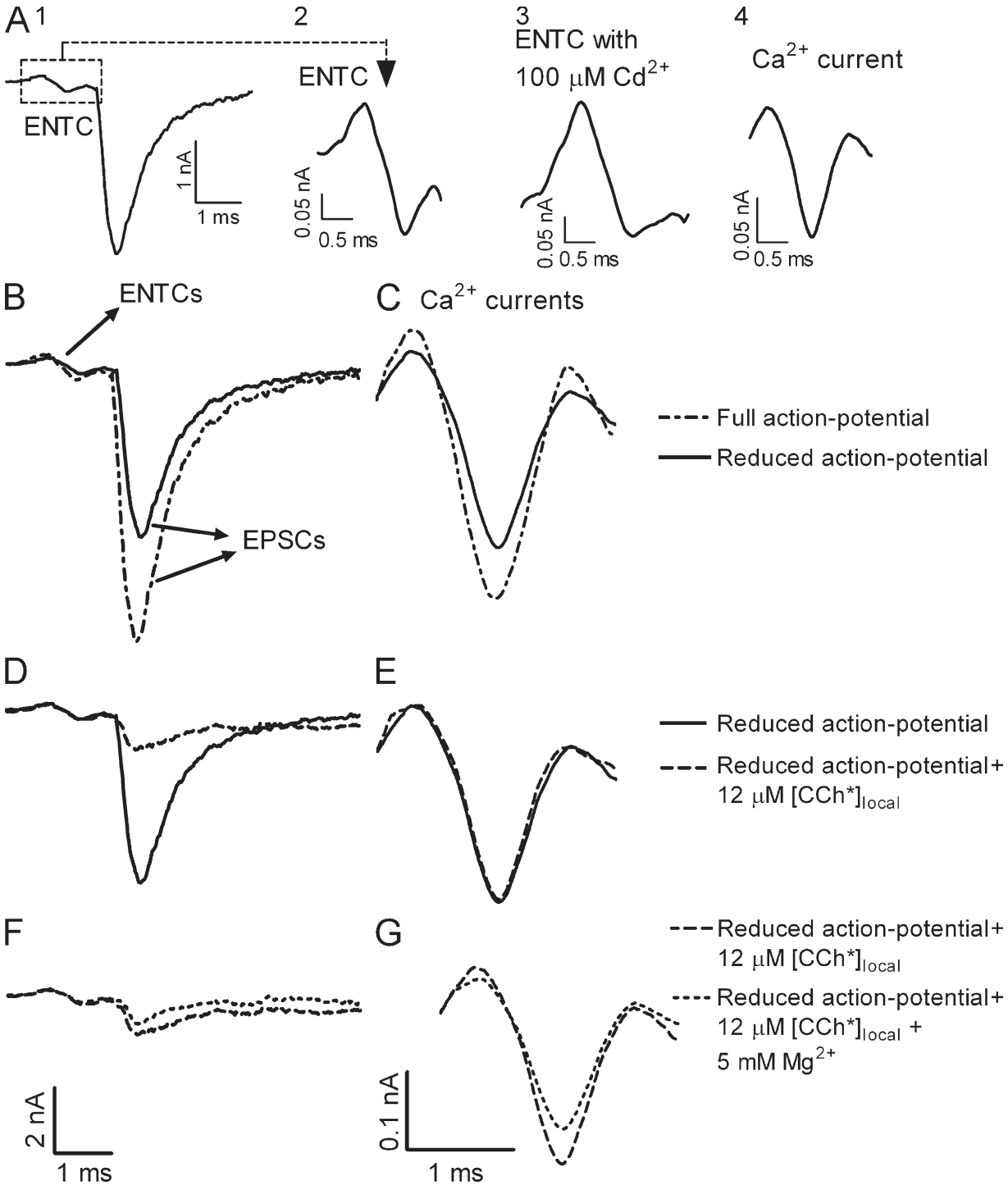

Figure 2. **[CCh*]$_{local}$ does not affect Ca^{2+} currents.** (A) Experimental protocol. (A_1) The ENTC (dashed square) and the resultant EPSC. (A_2) The ENTC on a larger scale. (A_3) The ENTC after addition of 100 μM Cd^{2+}. (A_4) Net Ca^{2+} current obtained after subtracting the current seen in A_3 from the ENTC. (B–G) Bars in the bottom of each column apply to that entire column. (B and C) Representative example (n = 3) of ENTCs and EPSCs (B) and Ca^{2+} currents (C) measured with a full action potential (dashed line) and with 50 nM TTX (solid line; i.e., smaller action potential). (D–G) In the presence of 50 nM TTX. (D and E) Representative example (n = 5) of ENTCs and EPSCs (D) and Ca^{2+} currents (E) measured before (solid line) and 1 ms after (dashed line) the flash ([CCh*]$_{local}$ = 12 μM). [CCh*]$_{local}$ reduced release to 19% of control without affecting Ca^{2+} currents. (F and G) ENTCs and EPSCs (F) and Ca^{2+} currents (G) with the same flash in normal $[Mg^{2+}]_o$ (1 mM; long dashed line) and with elevated $[Mg^{2+}]_o$ (5 mM; short dashed line). Representative example, n = 3.

currents to 82% of control (Fig. 2 G). The EPSC was reduced, much more, to 57% of control (Fig. 2 F). The results of Fig. 2 support the conclusion that the flash-induced reduction in release seen in Fig. 1 cannot be attributed to CCh-mediated inhibition of Ca^{2+} currents.

The M_2R allosteric antagonist gallamine inhibits M_2R GCs and reduces ACh release

The rapid effect (within 1–3 ms) of [CCh*]$_{local}$ on both the GCs and ACh release and the good correlation between inhibition of GCs and reduction of release suggests a causal relationship

between GCs and release. It is, however, possible that this correlation is fortuitous. $[CCh^*]_{local}$ could activate G protein to form $G_{\beta\gamma}$. $G_{\beta\gamma}$, in turn, could reduce release by acting directly on the release machinery (Blackmer et al., 2005). To test whether $G_{\beta\gamma}$ mediates the rapid flash-induced reduction of release we sought an M_2R ligand that inhibits the GCs but does not activate the G protein, hence $G_{\beta\gamma}$ will not be formed. We noticed that the $IC_{50\text{-}GCs}$ (1.34 ± 0.10 µM) was ten times higher than the apparent K_d (0.1 ± 0.01 µM) of the M_2R-mediated G protein–activated inwardly rectifying K^+ (GIRK) currents (Fig. S2). This suggests that the GCs are inhibited by ligands binding to a site other than the orthosteric one, possibly an allosteric site, which is known to exist in the M_2R (Conn et al., 2009). Gallamine (Gal), an M_2R-specific allosteric ligand (Lee and el-Fakahany, 1991), was shown (excluding one study [Jakubík et al., 1996]) not to activate G protein cascades (Gregory et al., 2007). We first examined whether also under our experimental conditions Gal did not activate G protein to form $G_{\beta\gamma}$. To do so we examined whether Gal induces GIRK currents, which are known to be induced by $G_{\beta\gamma}$ (Dascal, 1997). We found that the highest concentration of Gal used in our experiments (5 µM) did not produce any detectable GIRK current. Satisfied with this result, we tested the effect of Gal on M_2R GCs and on ACh release. At higher than −40 mV, Gal affected the On response of the GCs in a voltage-dependent manner, suggesting that the On response is contaminated by currents other than GCs. Thus, to isolate the effect of Gal on the GCs alone we altered the pulse protocol (Fig. 3 A, inset). We used pulses from −120 mV to −40 mV, where the On and the Off responses are the same, ensuring that only GCs are measured. Fig. 3 A shows that Gal inhibited M_2R GCs dose dependently. The DI_{GCs} curve compiled from experiments as in Fig. 3 A shows an $IC_{50\text{-}GCs}$ of 0.89 ± 0.05 µM (Fig. 3 B).

Next, we tested the effect of Gal on ACh release. Fig. 3 C shows that increasing Gal concentration, up to 5 µM, decreased the EPSC in a dose-dependent manner. To the best of our knowledge, this is the first demonstration that Gal at such low concentrations decreases evoked release. At much higher concentrations (200 µM) Gal may increase release (Katz and Miledi, 1978). Gal is known to have various postsynaptic inhibitory effects (Mitchelson, 1988). Thus, the reduction in the EPSC could be attributed to these effects. However, the Gal-induced reduction of release seen here is likely to be of presynaptic origin, as Gal did not change the quantum size (Fig. 3 C, "x" symbols). Furthermore, evaluation of the quantal content using the failure method (Martin, 1966; a method that is invariant to the size of the EPSC) or by dividing the average EPSC size by the average quantum size (Martin, 1966) provided similar results (Fig. 3 D). Gal could reduce release by decreasing Ca^{2+} currents. However, 10 µM Gal did not reduce Ca^{2+} currents (Fig. 3 E). Gal was shown to bind also nicotinic receptors (Loiacono et al., 1993), hence presynaptic nicotinic receptors (Wonnacott, 1997) could mediate the Gal-induced reduction of release seen here. This possibility can be ruled out as Gal had no effect on the EPSC in M_2KO mice (Fig. 3 F). We next examined whether Gal-mediated inhibition of GCs correlates with Gal-mediated reduction in release. To do so, we constructed a $DI_{release}$ curve, compiled from data such as those seen in Fig. 3 C, and compared it to the DI_{GCs} curve (taken from Fig. 3 B). Fig. 3 G shows a good correlation between the two curves; the $IC_{50\text{-}release}$ was 0.85 ± 0.07 µM and the $IC_{50\text{-}GCs}$ was 0.89 ± 0.05. To further support the conclusion that it is the inhibition of the GCs that is responsible for the Gal-induced reduction in ACh release we measured the effect of Gal on the rate of spontaneous release. Gal should not affect spontaneous release as there, the GCs are not relevant. Fig. 3 H shows that the rate of spontaneous release was not altered even when 5 µM Gal was applied, a concentration that reduced evoked release to ∼24% of control.

The tight correlation between the inhibition of GCs and reduction of release induced by the allosteric ligand Gal support the conclusion that the flash-induced reduction of release is not mediated by $G_{\beta\gamma}$ and is compatible with the notion of causal relationship between GCs in the M_2R and release of ACh.

The Gal-induced reduction of ACh release seems to contradict data showing that methoctramine (Meth), a competitive M_2R antagonist, increases ACh release (Slutsky et al., 2001). A possible explanation for this discrepancy could be that Gal, being a noncompetitive allosteric antagonist, reduces release due to its inhibition of the GCs whereas Meth could increase release because it displaces ACh from the M_2R and consequently relieves the tonic block of release that requires ACh binding to the M_2R. Alternatively, Meth could increase release by increasing the GCs, thus facilitating removal of the tonic block. To check for these possibilities we conducted a series of experiments summarized in Fig. S3. We found, to our surprise, that Meth inhibited the GCs in the M_2R but increased, as was already shown (Slutsky et al., 2001), both spontaneous and evoked release. However, when Meth was co-applied with a concentration of ACh that counteracted the enhancing effect of Meth on spontaneous release, surprising results were obtained. ACh inhibited release and ACh +Meth inhibited release even further (Fig. S3 D, compare dashed and green lines). The same was observed when a flash of CCh was applied instead of steady-state ACh (Fig. S3 E). Thus, the results of Fig. S3 support the notion that although Gal reduces release by inhibiting the GCs, Meth alone enhances release because it replaces ACh binding to the GPCR, hence alleviating the tonic block. Because Meth does not activate M_2R-coupled G protein (Daeffler et al., 1999), the conclusion that the reduction in release seen with CCh, Gal, and Meth (+ACh) is due to inhibition of the GCs is further supported.

The flash of CCh reduces release only if applied before or during the depolarizing pulse

To further support the linkage between GCs in the M_2R and release of ACh we designed yet another experimental protocol. If it is indeed inhibition of the GCs that reduces release, then the flash is expected to reduce release only if given shortly before or at the time that the GCs are produced, i.e., before or during the depolarizing pulse, but not after depolarization. To check for this possibility, we kept the concentration of CCh produced by the flash fixed but changed the timing of the flash relative to the 0.2-ms test pulse. That is, the flash was administered 1 ms before, in the middle of, or 0.05 ms after the test pulse (Fig. 4). In this way, the same $[CCh^*]_{local}$ (4 µM) encountered full, partial,

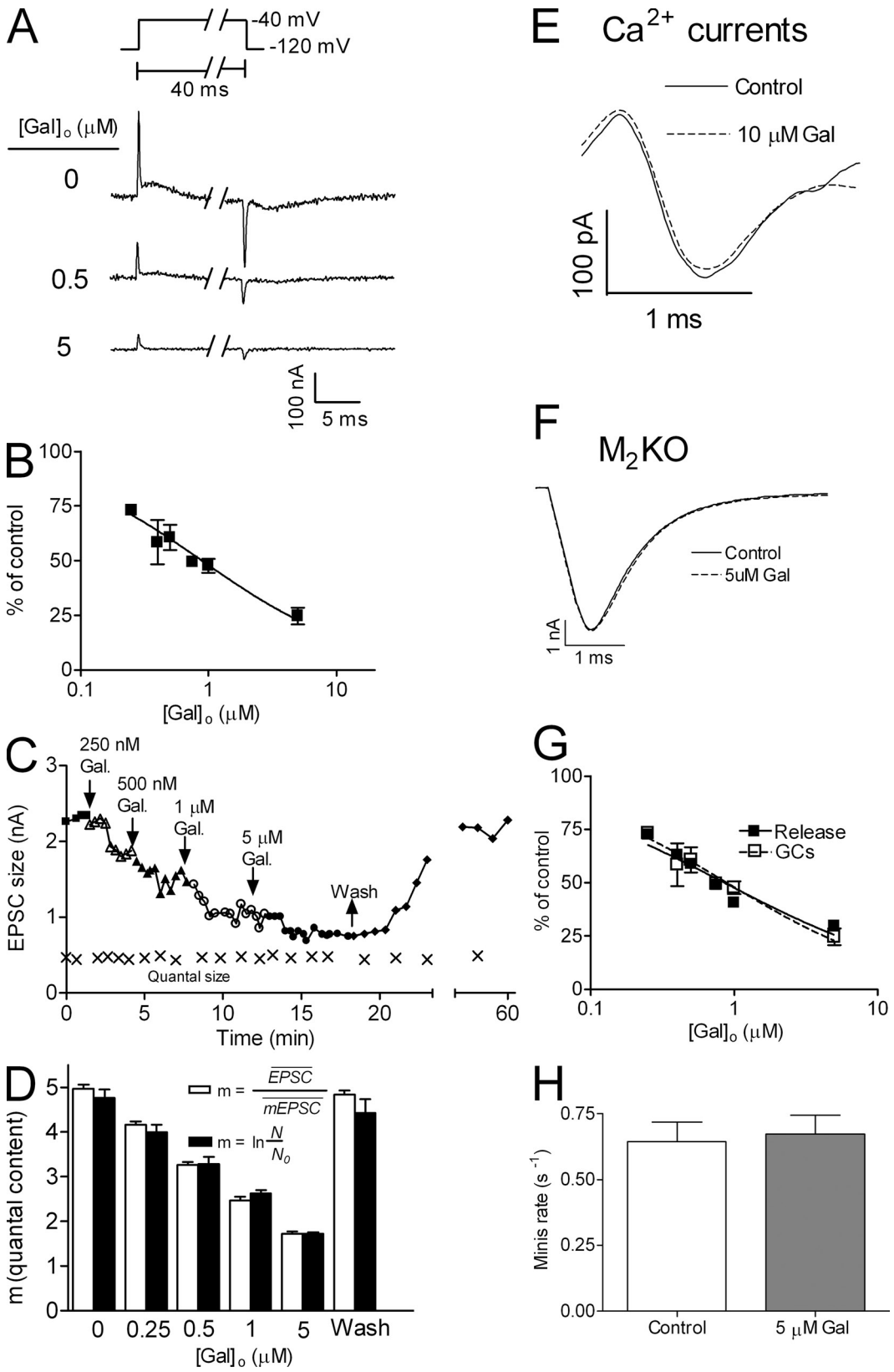

Figure 3. **Gal inhibited the GCs and reduced ACh release.** (A) Samples of GCs induced by depolarizing the oocyte from −120 mV to −40 mV at different concentrations of Gal. Inset shows the pulse protocol. (B) Normalized DI_{GCs} curves for Gal. In each oocyte, GCs were measured in control and with one concentration of Gal (n = 4–10 for each point taken from 6 donors). $IC_{50\text{-}GCs}$ = 0.89 ± 0.05 µM. (C) A representative experiment depicting the dose-dependent effect of Gal on the EPSC size. Washing Gal restored the control values of the EPSC. The quantum size (×), monitored throughout the experiment by measuring the size of asynchronous single quanta released more than 50 ms after depolarization, remained constant. (D) Evaluation of the quantal content (m) from $m = \frac{\overline{EPSC}}{\overline{mEPSC}}$ (empty bars), where $\overline{EPSC}$ is the average EPSC and $\overline{mEPSC}$ is the average size of a single quantum, and from $m = \ln\frac{N}{N_0}$

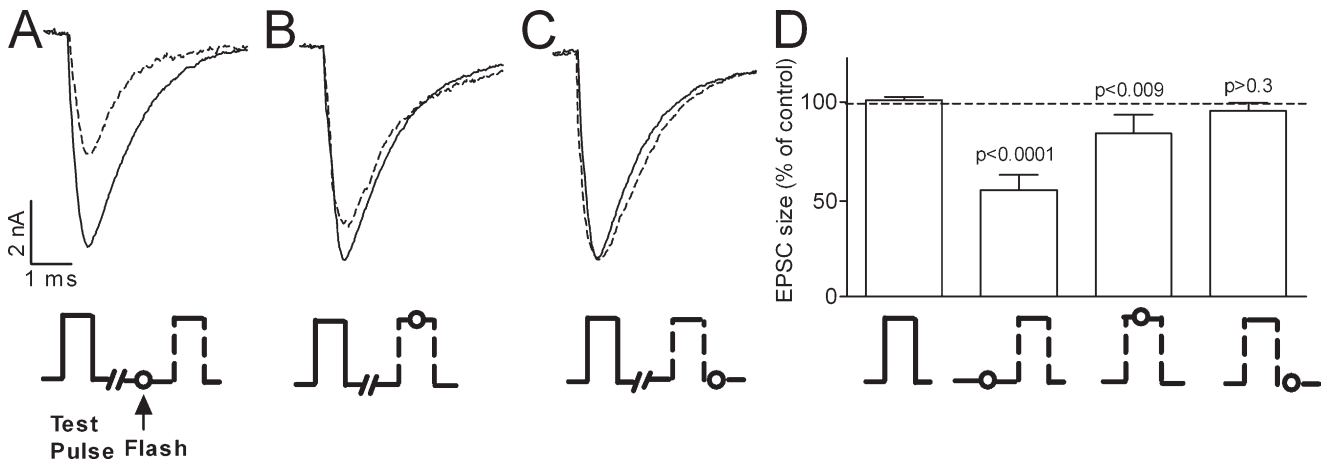

Figure 4. **The flash reduced release only if applied before or during the depolarizing pulse.** $[CCh^*]_{local}$ = 4 µM. $[TTX]_o$ = 0.5 µM. Experimental protocols beneath EPSCs and corresponding columns. EPSCs without (solid line) and with (dashed line) flash. (A–C) Same site, each trace is an average of five repetitions. Test pulse, −1.0 µA, 0.2 ms. Flash was applied 1 ms before (A), in the middle of (B), and 0.05 ms after (C) the test pulse. (D) Average of 14 experiments as in A–C. From left to right, 100 ± 2%, 54 ± 2%, 83 ± 5%, and 97.5 ± 4% of control (significance indicated above bars).

and no GCs, respectively. Because exact timing of the flash with respect to the depolarizing pulse was crucial, we used focal depolarization instead of an action potential to induce release. The results of Fig. 4 clearly show that the flash reduced release only when applied before or at the time that the GCs were produced. Maximal reduction of release (54 ± 2% of control) was seen when the inhibition of GCs was presumably the largest, i.e., when the flash was applied shortly before the test pulse (Fig. 4, A and D). No reduction in release (97.5 ± 4% of control) was seen when presumably no inhibition of GCs took place, i.e., when the flash was applied after the test pulse (Fig. 4, C and D). An intermediate effect was obtained (release was 83 ± 5% of control) when partial inhibition of the GCs presumably took place, i.e., when the flash was applied in the middle of the test pulse (Fig. 4, B and D). This intermediate effect could be accounted for by the ∼0.2-ms time constant of the fast component of the GCs (Ben-Chaim et al., 2006). That is, with the $t_{1/2}$ of uncaging being ∼40 µs (Milburn et al., 1989), $[CCh^*]_{local}$ was elevated soon after the flash and thus encountered a fraction of the GCs that occurred during the second half of the 0.2-ms test pulse.

The finding that the flash reduced release to 83% of control when given during the depolarizing pulse and had no effect when applied 0.15 ms later further supports the notion of causal relationship between the GCs and release. This result refutes once again the possibility that $G_{\beta\gamma}$ is involved in the flash-induced reduction of release because the same amount of $G_{\beta\gamma}$ is expected to be produced if the flash is given 0.15 ms later. Furthermore, the finding that the flash given during the 0.2-ms pulse was effective in reducing release implies that binding of CCh to the GPCR and the subsequent inhibition of the GCs takes place with a time constant of tens of microseconds.

The amount of ACh release is controlled by both Ca^{2+} and by M_2R GCs

The quantal content is known to depend on Ca^{2+} (Dodge and Rahamimoff, 1967). Our results suggest that also the GCs affect the quantal content. We thus examined the relative contribution of Ca^{2+} and GCs in determining the quantal content. To do so, one needs to keep one of the factors constant and vary the other; i.e., fixed GCs and variable Ca^{2+} and vice versa. This cannot be achieved by varying the depolarization level, as the latter affects both. We thus used a constant action potential and changed $[Ca^{2+}]_o$. The GCs were modulated by varying $[CCh^*]_{local}$. For each $[CCh^*]_{local}$ we measured the dependence of the size of the EPSC on $[Ca^{2+}]_o$. Fig. S4 A shows that, as is well documented (Dodge and Rahamimoff, 1967), the quantal content rose as $[Ca^{2+}]_o$ increased, and leveled off near the physiological $[Ca^{2+}]_o$ (2 mM). However, we made the novel observation that release also increased as the GCs rose. This can also be seen when release is plotted as a function of GCs (expressed as a fraction of control GCs) in different $[Ca^{2+}]_o$ (Fig. S4 B). The finding that the maximal quantal content increased as the GCs increased (Fig. S4 A) suggests that under physiological conditions (action potential and 2 mM $[Ca^{2+}]_o$) it is the GCs produced during the action potential, together with Ca^{2+} that had entered, that determine the quantal content.

The effect of the flash on release is cancelled when its application is preceded by a prepulse that generates GCs without eliciting detectable Ca^{2+} influx

Up to this point, the GCs were produced by the same depolarizing pulse that also admitted Ca^{2+} and consequently evoked release. To unravel the intrinsic contribution of GCs to release there is a

(full bars), where *N* is the number of pulses applied and N_0 is the number of failures. As seen, the two methods produced similar values of m (*n* = 6). (E) Ca^{2+} currents without (solid line) and with (dashed line) 10 µM Gal (representative experiment, *n* = 3). (F) Superimposed average EPSCs (*n* = 5) recorded in M_2KO mice in control (solid line) and with 5 µM Gal (dashed line). (G) $DI_{release}$ curve (■, *n* = 8) for Gal constructed from experiments such as those in C ($IC_{50\text{-release}}$ = 0.85 ± 0.07 µM) compared with the DI_{GCs} curve of Gal (taken from B). (H) Rate of spontaneous release (in WT mice) in control (white), and with 5 µM Gal (gray; *n* = 5).

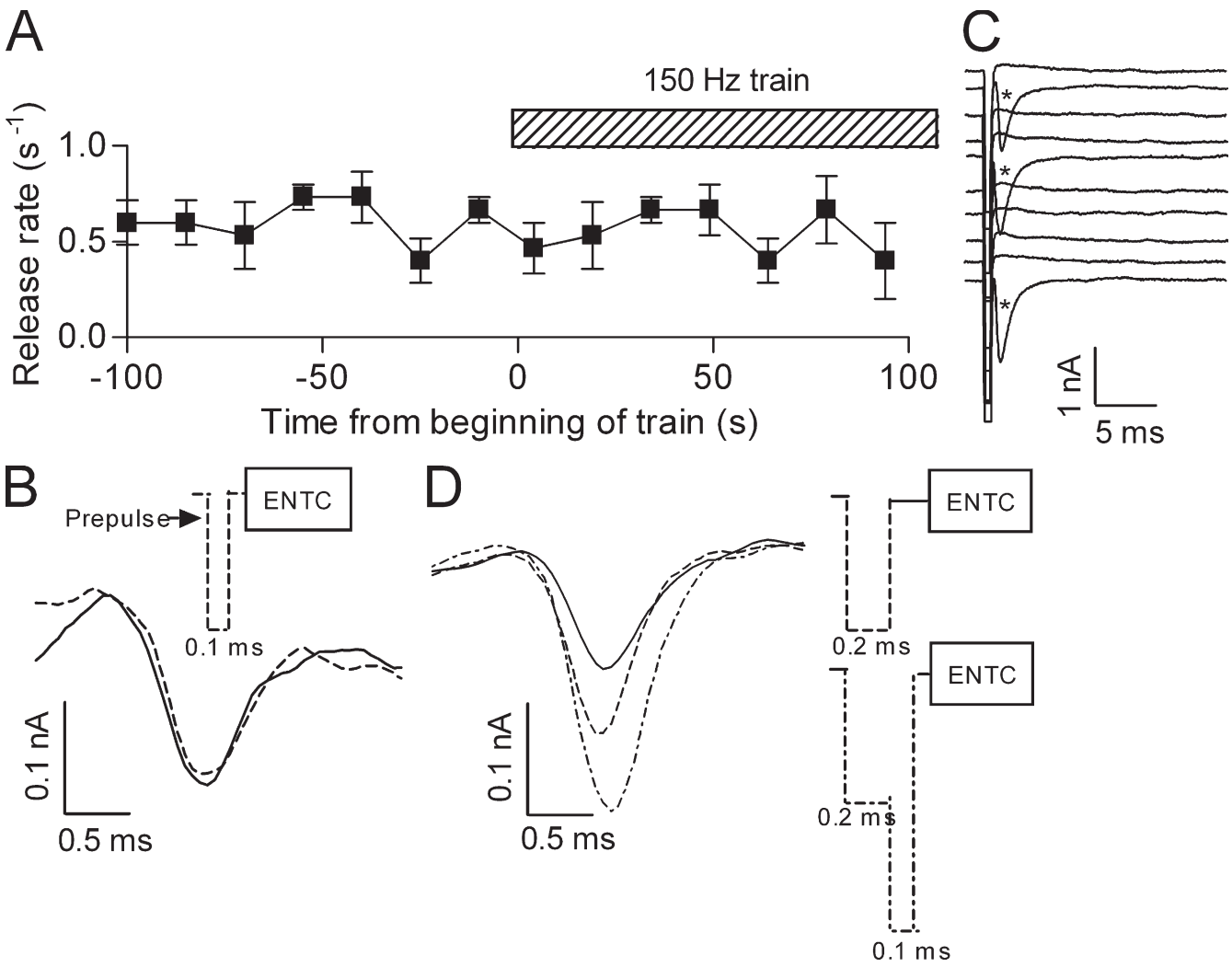

Figure 5. **The brief (0.1 ms) and strong (−1.0 µA) prepulse does not admit Ca^{2+}.** (A) The rate of release during a train (150 Hz, 100 s) of brief "prepulses" (dashed bar) was similar to that of spontaneous release before the train (■, compare rate before and during the train; *n* = 5). (B) Representative (*n* = 4) Ca^{2+} currents derived from ENTCs without (solid line) and with (dashed line) the brief prepulse preceding the ENTC. Inset shows experimental protocol. (C) Representative traces (without selection) showing evoked release (*) produced by a wider (0.2 ms, −1.0 µA) prepulse. (D) Representative (*n* = 4) Ca^{2+} currents derived from ENTCs without (solid line), with the wider prepulse (long dashed line), and with the wider prepulse followed immediately by even stronger (−2.0 µA, 0.1 ms) depolarization (short dashed line). Here and in B the prepulses were given such that they terminated 0.15 ms before the ENTC. Inset shows experimental protocols.

need to separate between the generation of the GCs and the induction of release. To this end, we designed experiments where depolarization induced GCs but not release and then examined the effect of modulation of the GCs alone on release produced by a separate depolarizing pulse. From our previous work (Parnas et al., 2005; Kupchik et al., 2008; and see Fig. 5 A) we know that an extremely brief (0.1 ms) but strong (−1.0 µA) depolarizing prepulse does not evoke release, suggesting that it does not admit Ca^{2+}. Yet such a prepulse enhances release when it precedes, by a few milliseconds, a wider test pulse. We posit that such a prepulse is actually a pure source of GCs. We can therefore apply the flash before or after the prepulse, thereby modulating only the GCs, and hence examine directly the effect of the GCs on release produced by a following test pulse.

We first tested directly our assumption that the brief prepulse does not admit Ca^{2+} in detectable amounts. To do so we used two criteria: we measured whether a train of prepulses evoked ACh release and whether the prepulse itself produced Ca^{2+} currents. To check for release, we administered the prepulse at high frequency (150 Hz) for 100 s and measured release during the train. Fig. 5 A shows that the rate of release (~0.5 s^{-1}) during the train was the same as the rate of spontaneous release before the train. Furthermore, release during the train occurred randomly and was not locked to the pulse. These results suggest that Ca^{2+} did not accumulate to an appreciable level even during the high frequency train of stimulation. In addition, we tried to measure directly Ca^{2+} currents produced by the prepulse. Based on the results of Fig. 5 A we suspected that even if the prepulse produces Ca^{2+} currents they will be too small to be detected. However, if the prepulse will closely precede an ENTC, then the putative "prepulse-Ca^{2+} currents" will add to the "ENTC-Ca^{2+} currents" and the chance to detect them will increase. Fig. 5 B shows the results of such an experiment. It is seen that the brief prepulse (0.1 ms) did not affect the ENTC-Ca^{2+} currents.

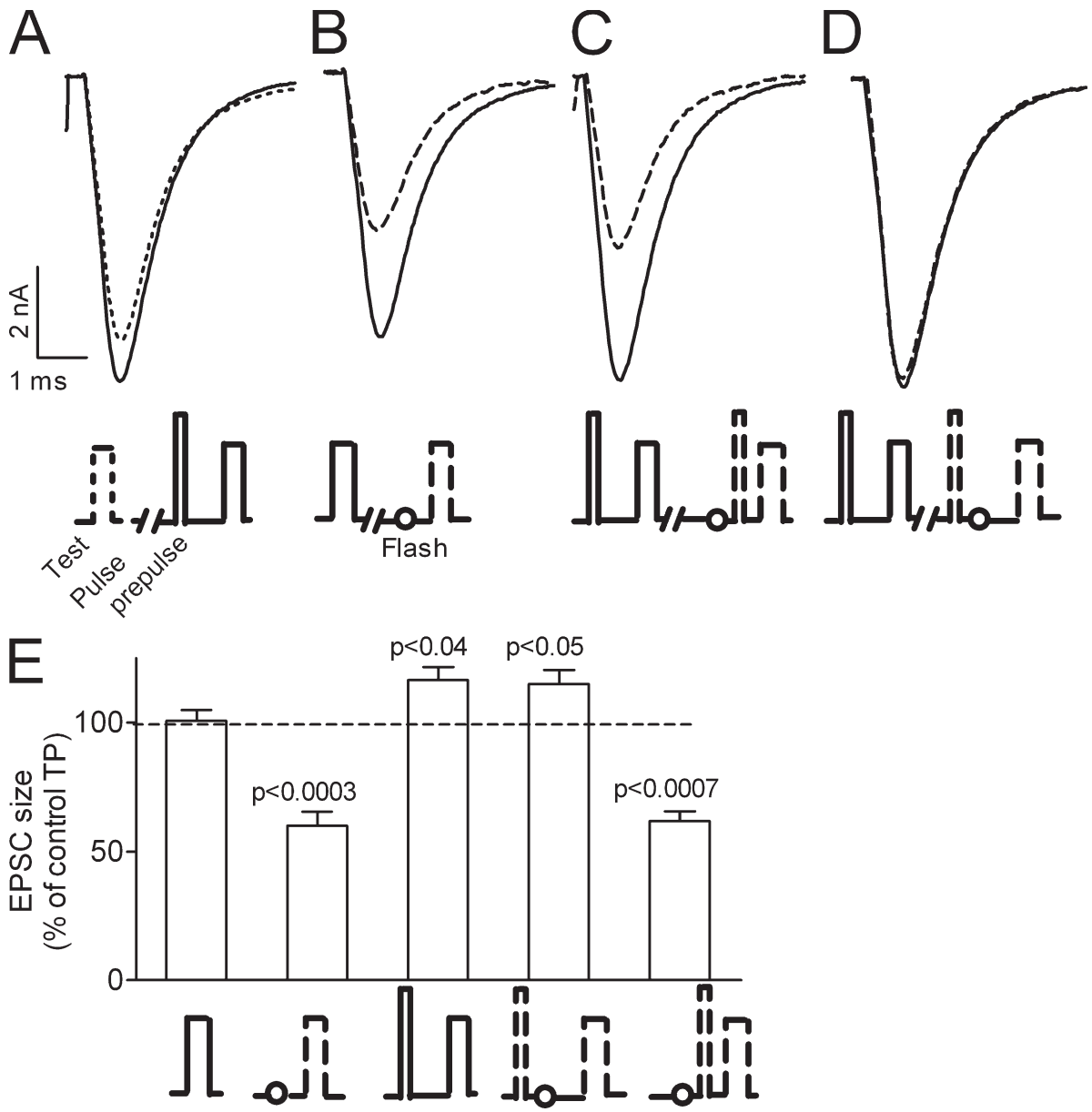

Figure 6. **The effect of the flash is prevented if it is preceded by the very brief (0.1 ms) and strong (−1.0 μA) prepulse.** (A–D) Test pulse (−0.6 μA, 0.2 ms) EPSCs under various conditions. Recordings from the same site, each trace is an average of five repetitions. Flash was always applied 1 ms before the test pulse. (A) The test pulse is preceded by 1.2 ms (solid line) or not (dashed line) by the prepulse. (B–D) EPSCs without (solid line) and with (dashed line) a flash. (B) The test pulse alone and preceded by the flash. (C) The flash precedes the prepulse by 0.2 ms. (D) The flash follows the prepulse by 0.2 ms. (E) Average of 14 experiments as in A–D. From left to right, 100 ± 4%, 60 ± 5%, 117 ± 5%, 115 ± 5%, and 62 ± 4% of control.

To assure that this method can detect Ca^{2+} currents preceding the ENTC if they do occur, we repeated this experiment but with a wider (0.2 ms) prepulse that by itself did produce release (Fig. 5 C). The wider prepulse increased the ENTC-Ca^{2+} currents and the increase was leveled off toward the end of the current (Fig. 5 D). These results could be explained as follows. The prepulse could have affected the dynamics of the Ca^{2+} channels. Alternatively, because the 0.2-ms prepulse is strong (−1.0 μA), Ca^{2+} is likely to enter mainly as a tail current (Llinás et al., 1981). These tail currents begin before the ENTC-Ca^{2+} currents and hence presumably add to them. To check whether the latter explanation holds, we administered immediately after the prepulse a brief (0.1 ms) and even stronger (−2.0 μA) depolarization, which is expected to be closer to the reversal potential of Ca^{2+}. Under these conditions it is expected that the tail currents will now begin 0.1 ms later and hence the increase in the ENTC-Ca^{2+} currents will be extended to later parts of the ENTC-Ca^{2+} currents. Indeed, Fig. 5 D shows that this is the case. Thus, although we cannot exclude an effect on Ca^{2+} channels, we may conclude that the 0.2-ms prepulse did admit Ca^{2+} whereas the 0.1-ms prepulse did not admit Ca^{2+} to an appreciable level.

We can now isolate the intrinsic contribution of the GCs to release. To do so, the flash was given, as before, 1 ms before the test pulse, whereas the prepulse either preceded or followed the flash by 0.2 ms. When the flash is given after the prepulse it is not

expected to affect the GCs that were already produced by the prepulse. Hence, it is not expected to abolish the enhancing effect of the prepulse on release. In the opposite case when the flash is given before the prepulse, it is expected to inhibit the prepulse-induced GCs and reduce, or even completely abolish, the enhancing effect of the prepulse on test pulse release. With this protocol we could ask directly whether the GCs produced during the prepulse affect test pulse–evoked release. As seen in earlier studies (Parnas et al., 2005; Kupchik et al., 2008), the prepulse enhanced test pulse release (Fig. 6, A and E, third column). When the flash was given before the prepulse it had a dual effect. It abolished the prepulse-induced enhancement of test pulse release and as before (Fig. 1 D) reduced test pulse release. The dual effect is evident as this flash reduced the EPSC to 62 ± 4% of control (Fig. 6, C and E, rightmost column), a similar reduction as that obtained without a prepulse (Fig. 6, B and E, second column). In this case, the flash inhibited both the prepulse-induced and the test pulse–induced GCs. In contrast, when the flash was given after the prepulse but before the test pulse it did not prevent, as predicted, the prepulse-induced enhancement of release. Surprisingly, it also did not reduce test pulse release (Fig. 6, D and E, compare third and fourth columns).

The findings that when a flash was given 1 ms before a test pulse it did reduce release (Fig. 1) and when it was given after the prepulse but still 1 ms before the test pulse it did not reduce release seem puzzling. The puzzle may be solved in the framework of our hypothesis and earlier studies. As detailed in the Introduction, we suggest that at resting potential the release machinery is under tonic block imposed by the controlling GPCR. Release initiates when upon depolarization the tonic block is alleviated (Parnas and Parnas, 2007). This notion was tested and validated experimentally (Parnas et al., 2005; Kupchik et al., 2008). It was further shown that once freed the release machinery remains free for ∼2–4 ms (Parnas et al., 2005). Referring to the present results, on the assumption that the release machinery was freed by the prepulse-induced GCs it will still remain free 1.2 ms later when the test pulse is applied. Therefore, the flash given after the prepulse is irrelevant, as the release machinery is already freed by the prepulse. In this case, the flash is not expected to reduce release itself, nor is it expected to abolish prepulse-induced enhancement of test pulse release.

The timing of initiation of release is governed by the GCs

Finally, we examined whether GCs affect release initiation. We recall that accumulation of Ca^{2+} before depolarization increased the quantal content but did not cause release to start earlier (Datyner and Gage, 1980; Slutsky et al., 2003), compatible with the notion that it is not Ca^{2+} that determines the onset of release (Parnas and Parnas, 2007). If the GC-induced alleviation of the tonic block of release triggers release, then we expect that if the GCs are induced already before the test pulse, before test pulse–induced Ca^{2+} influx, then test pulse release should start sooner. To check for this possibility we exploited the finding that the high and brief prepulse does not admit Ca^{2+} (Fig. 5) and hence is likely to be a pure source of GCs. We used a low test pulse that produced mostly single quanta events and thus could construct a synaptic delay histogram, which reflects the time course of release (Katz and Miledi, 1965). The prepulse was applied before every other test pulse, thus delay histograms of release evoked by the test pulse alone or by the test pulse preceded by the prepulse were constructed simultaneously (Fig. 7, A and B). Presenting the delay histograms on a fast time scale reveals that in WT mice (Fig. 7, A_2) test pulse release started significantly earlier when the test pulse was preceded by the prepulse. The effect of the prepulse was abolished by Gal (Fig. 7 A, insets). Acknowledging that only the test pulse admits Ca^{2+}, the results in Fig. 7 A suggest that initiation of test pulse release was determined by the GCs produced during the prepulse. Not surprisingly, in M_2KO mice, where release is not under tonic block, the prepulse had no effect on release, in particular its initiation (Fig. 7 B).

The results of Fig. 7, A and B, may be used to unravel the temporal sequence of the two processes induced by the action potential (Fig. 7 E). Superposition of the delay histogram obtained in WT mice when a prepulse was applied with the delay histogram of M_2KO mice shows that the two curves overlap. In these two cases the release machinery was free when the test pulse was applied; that is, release initiation was presumably governed by Ca^{2+} influx. This point in time thus correlates with activation of the exocytotic machinery due to Ca^{2+} influx. The point in time where the GC-mediated removal of the tonic block (brake) takes place is deduced from the time of initiation of release in WT mice, without a prepulse. As seen (Fig. 7 E), in this case release started later than in M_2KO mice and in WT mice with a prepulse. Hence, we suggest that the GC-induced removal of the brake triggers physiological depolarization-evoked Ca^{2+}-dependent neurotransmitter release.

In contrast to the brief (0.1 ms) and strong (−1.0 µA) prepulse, a low (−0.2 µA) but wide (0.9 ms) prepulse admitted Ca^{2+} (Fig.7 C_1, inset) and, as expected, induced release (although to a very low level; Fig. 7 C_1, dotted line). This wide prepulse increased test pulse release to a similar extent as that produced by the strong and brief prepulse (compare Fig. 7 C_1 to Fig. 7 A_1). However, unlike the strong and brief prepulse, the wide and low prepulse did not cause release to initiate earlier (Fig. 7 C_2). Recalling that the brief prepulse induces GCs in the M_2R without admitting Ca^{2+} and the wide prepulse does admit Ca^{2+}, this result supports the notion that initiation of release is determined by the GCs and not by Ca^{2+} influx. In addition, the wide prepulse, again in contrast to the brief one, caused release to initiate earlier in M_2KO mice (Fig. 7 D). This is not surprising, as in the M_2KO mice the release machinery is presumably constantly free, hence, initiation of release correlates with influx of Ca^{2+}. Thus, as Ca^{2+} enters already during the wide prepulse, test pulse release is expected, as is indeed the case, to begin earlier.

Discussion

We presented here a novel mechanism for GPCR-mediated signal transduction. GPCRs control most signal transduction processes (Hamm, 1998; Gether, 2000). They do so by binding of an agonist, which in turn activates their coupled G protein. We used depolarization-evoked release of neurotransmitter, whose kinetics is controlled by GPCRs (Parnas and Parnas, 2007), as

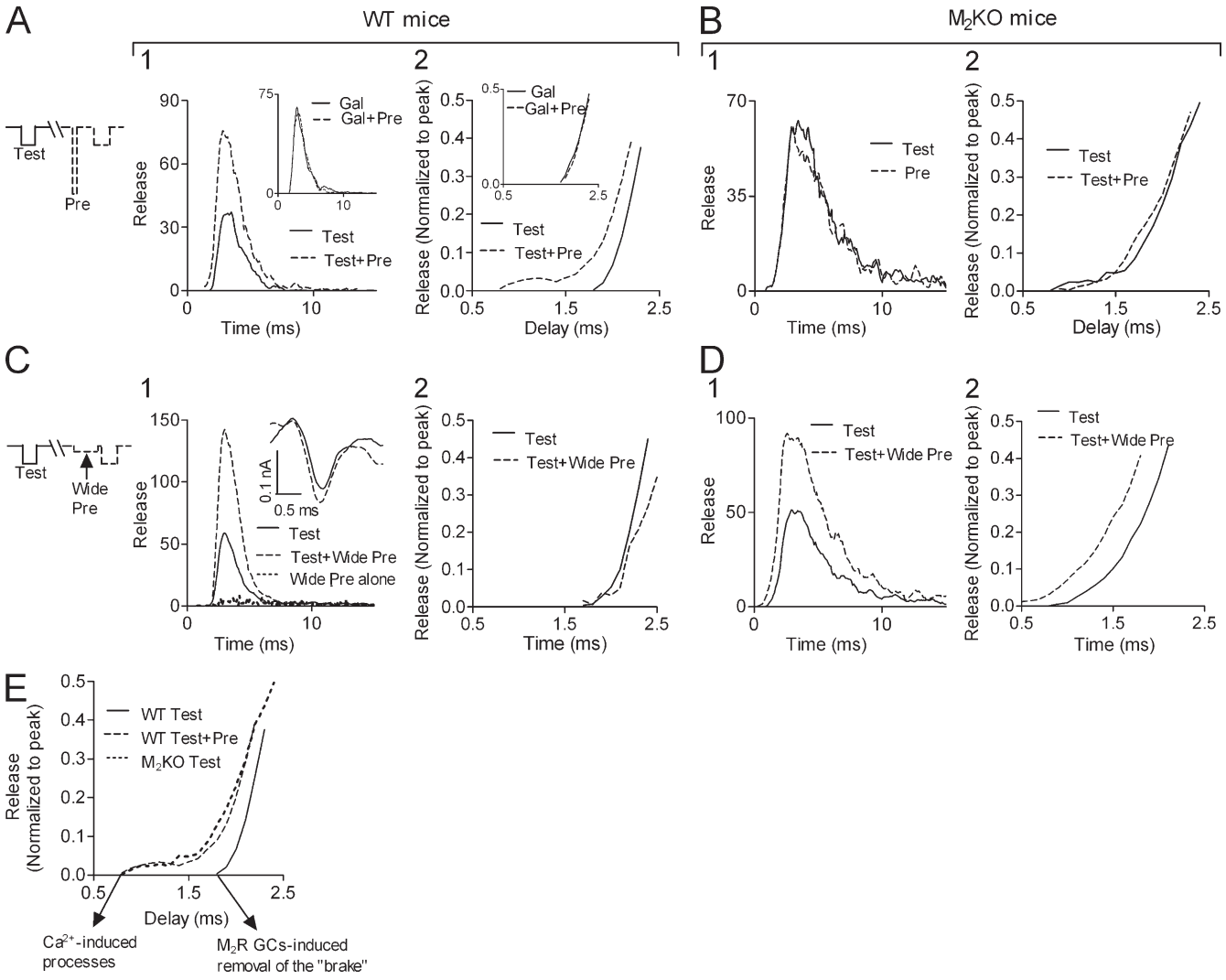

Figure 7. **Initiation of depolarization-evoked release depends on the timing of the GCs.** Experiments performed at 10°C (n = 4–5 for each histogram). Protocols shown on the left of each row correspond to the entire row. Test = test pulse (−0.5 μA, 0.5 ms); Pre = prepulse (−1.0 μA, 0.1 ms); Wide pre = wide prepulse (−0.2 μA, 0.9 ms). (A) In WT mice, application of the prepulse 1 ms before the test pulse increased the amount of release (A_1) and caused release to initiate earlier (A_2, Kolmogorov-Smirnov [KS] test, $P < 0.03$). Gal (insets) abolished the effect of the prepulse on release. (B) In M_2KO mice the strong and brief prepulse did not affect the amount (B_1) or the initiation (B_2) of release ($P > 0.9$). (C) In WT mice, application of a wide prepulse, which causes release by itself (C_1, short dashed line), increased the amount of test pulse release (C_1) but did not affect initiation of release (C_2, $P > 0.9$). Inset shows representative (n = 3) Ca^{2+} currents derived from ENTCs without (solid line) and with (dashed line) the wide prepulse preceding the ENTC. (D) In M_2KO mice, the wide prepulse increased the amount of release (D_1) and caused release to initiate earlier (D_2, $P = 0.008$). (E) Initiation of test pulse release in WT mice without (solid line) and with (dashed line) the brief and strong prepulse and in M_2KO mice without a prepulse (short dashed line) shown on the same axes.

an example of GPCR-mediated signal transduction. We presented here the first example where depolarization-induced charge movement in the GPCR controls the signal transduction. This novel mechanism enables extremely fast (in the range of hundreds of microseconds) signal transduction.

The evidence for the role of Ca^{2+} in the release of neurotransmitter is overwhelming and dates as far back as 1954 (Del Castillo and Katz, 1954). The classical Ca^{2+} hypothesis for neurotransmitter release is based on this evidence. Accordingly, the action potential opens Ca^{2+} channels, and Ca^{2+} rapidly enters the terminal and quickly reaches a concentration in the vicinity of the release sites, which is sufficiently high to initiate the release process. Removal of Ca^{2+} from near the release sites is responsible for termination of release (Neher and Sakaba, 2008). The Ca^{2+} hypothesis accounts for major experimental findings, notable among them is the quantitative relationship between the amount of transmitter release (the quantal content) and the concentration of Ca^{2+}, either extracellular (Dodge and Rahamimoff, 1967) or intracellular (Schneggenburger and Neher, 2000; Felmy et al., 2003a). However, the Ca^{2+} hypothesis cannot accurately account for the kinetics of depolarization-evoked release, as treatments that promote faster accumulation of Ca^{2+} should cause an earlier onset of release and faster removal of Ca^{2+} should facilitate termination of release. Contrary to these predictions, it has been shown that the kinetics of depolarization-induced transmitter release does not depend on treatments affecting Ca^{2+} influx and its removal (Fig. 7; Andreu and Barrett, 1980; Datyner and Gage, 1980; Slutsky et al., 2003; Bollmann and Sakmann, 2005). Remarkably, when release is induced by Ca^{2+} uncaging, without depolarization, the kinetics of this release

does depend on treatments affecting the level of intracellular Ca^{2+} (Schneggenburger and Neher, 2000; Felmy et al., 2003b; Bollmann and Sakmann, 2005). This fundamental difference between depolarization-induced release and Ca^{2+}-induced release suggests that different mechanisms underlie these two modes of release.

What, then, does control the kinetics of depolarization-induced release? As detailed in the Introduction, we proposed that the presynaptic GPCRs that mediate feedback autoinhibition of release of a specific neurotransmitter also control its fast release (Khanin et al., 1997; Parnas et al., 2000). This hypothesis was verified regarding ACh release, where the M_2R mediates feedback autoinhibition of ACh release (Slutsky et al., 1999) and also controls the kinetics of ACh release (Slutsky et al., 2001, 2003). Similarly, mGluRs of group II mediate feedback inhibition of glutamate release (Kew et al., 2001) and an mGluR that resembles group II mGluRs controls the kinetics of glutamate release (Kupchik et al., 2008). We thus suggest that this is a general mechanism that applies to depolarization-induced release of other neurotransmitters. Accordingly, release of each type of transmitter is expected to be controlled by the presynaptic GPCR that mediates feedback autoinhibition of release of that particular transmitter.

A substantial amount of data had been accumulated supporting our hypothesis that voltage-sensitive GPCRs control action potential–induced neurotransmitter release (Parnas et al., 2000; Parnas and Parnas, 2007, 2010). However, the underlying molecular mechanism, in particular how the transmitter-bound GPCR-imposed brake is removed by depolarization, still remained to be clarified. We believe that this issue had been resolved in this study, hence we can now, based on the present and previous results, suggest a molecular-level mechanism by which voltage-sensitive GPCRs control the kinetics of neurotransmitter release (Video 1). Briefly, at resting potential the GPCRs are in their high affinity state, and hence are able to bind the neurotransmitter, which is, at rest, at low concentration. The neurotransmitter-bound GPCR imposes a tonic block, brake, of release. The action potential ignites two processes, the temporal sequence of which can be inferred from Fig. 7 E. It admits Ca^{2+}, which rapidly activates the release machinery, and it induces charge movement in the GPCR, which removes, slightly later, the brake. Only then can the Ca^{2+}-dependent exocytosis be executed.

Our hypothesis that under physiological conditions it is the depolarization-induced charge movement that triggers neurotransmitter release (depolarization-induced release) seems to be contradicted by experiments where release was induced by increasing $[Ca^{2+}]_i$ (Ca^{2+}-induced release) without a concomitant depolarization (Bollmann et al., 2000; Schneggenburger and Neher, 2000). However, by analyzing the molecular-level model (Yusim et al., 1999) of our hypothesis, we suggested a way to reconcile the seemingly conflicting evidence (Parnas et al., 2002). To do so, let us begin with spontaneous release, which occurs at resting potential. At resting potential $[Ca^{2+}]_i$ remains low because without depolarization no appreciable Ca^{2+} influx takes place. In addition, at resting potential most of the release machinery is blocked due to its association with the transmitter-bound high affinity GPCR (Video 1). However, rare spontaneous excursions occasionally permit a release event by freeing the release machinery from its association with the GPCR. In most models (Dodge and Rahamimoff, 1967; Schneggenburger and Neher, 2005; Pan and Zucker, 2009) it is assumed that Ca^{2+} interacts with an entity X to promote release. In our model (Lustig et al., 1989), X correlates with the free release machinery. Thus, during spontaneous release when $[Ca^{2+}]_i$ is low, an equilibrium is maintained between the blocked and free release machinery. When $[Ca^{2+}]_i$ is abruptly increased to high concentrations (as is the condition at Ca^{2+}-induced release), the high $[Ca^{2+}]_i$ shifts the quasi-equilibrium between the blocked and the free release machinery toward large free release machinery. Thus, we suggest that spontaneous release is governed by a subset of the molecular scheme of depolarization-induced release, under conditions of no depolarization and low $[Ca^{2+}]_i$. Ca^{2+}-induced release, we suggest, can be looked at as a manifestation of spontaneous release under conditions of high $[Ca^{2+}]_i$.

The Ca^{2+} hypothesis attributes control of release to one factor only, Ca^{2+}. Our results with M_2KO mice (Fig. 7; Slutsky et al., 2003) demonstrate a crucial shortcoming of the one-factor hypothesis. In M_2KO mice, where release is controlled by Ca^{2+} alone, the time course of release is not robust; it alters during repetitive stimulation and depends on the kinetics of Ca^{2+} influx and removal (Slutsky et al., 2003). Thus, the one-factor hypothesis cannot guarantee robust kinetics of release, which is crucial for proper brain function. On the other hand, our hypothesis of two factors controlling release guarantees robust kinetics of release with concomitant modulation of the amount of transmitter being released.

Materials and methods

Mice

1.5–3-mo-old Sabra mice or M_2KO mice (mixed genetic background [129J1XCF; 50%/50%]; Gomeza et al., 1999) and age-matched WT mice (obtained from Taconic) were used. Results obtained in the Sabra mice resembled those of the control WT mice. The diaphragm and its phrenic nerve were isolated and pinned in a small chamber (1 ml). The bathing solution was composed of (mM): 150 NaCl, 2.5 KCl, 1 $MgCl_2$, 25 $NaHCO_3$, 8 D(+)-glucose, and 2 $CaCl_2$. Temperature was kept at 23 ± 1°C (10 ± 1°C in Fig. 7) by circulating the fluid from a reservoir beaker (4 ml) to the bath through a heat exchanger. The solution in the reservoir beaker was continuously bubbled with 95% O_2/5% CO_2 . For local graded depolarization (Figs. 4–7), 0.5 µM TTX was added (Dudel, 1981; Slutsky et al., 2003). pH was adjusted to 7.4 with NaOH.

Focal stimulation and recording of EPSCs and of single quanta events

Macropatch electrodes (~20 µm in diameter, ~200 kΩ) were used for focal depolarization and recording (Dudel, 1981). With this technique the extracellular potential below the macropatch electrode is clamped to ground. The electrode is filled with the bathing solution. The macropatch technique allows depolarization of the patch of membrane under the electrode by shifting the extracellular potential to a negative value. This technique allows application of very brief pulses as membrane capacitance is not involved. The macropatch electrode was positioned on the surface of the muscle and was gently glided while applying depolarizing pulses (at 10 Hz) until postsynaptic single quanta responses with a fast rise time were detected. The same macropatch electrode served both to depolarize the terminal and at the same time record postsynaptic currents. When it was desired that the focal depolarization produce an action potential (Figs. 1–3), the amplitude of the depolarizing pulse was increased until an abrupt all-or-none jump in the size of the postsynaptic current was observed. Muscle contractions were prevented by addition of 50 nM TTX. Stimulus or flash artifacts always appeared before the EPSC. These artifacts were recorded separately and subtracted from the EPSC recordings offline. Subtracting the artifact did not affect the peak amplitude of the EPSCs.

In experiments involving flash photolysis or prepulses (see below) the EPSC was measured alternately without and with the flash/prepulse. This ensured that the EPSCs with and without the flash/prepulse were measured over the same period of time. Thus, possible time- or use-related distortions in EPSC amplitude were avoided.

Traces were digitized at a sampling rate of 50 kHz without filtering and saved on a personal computer using the LabView interface (National Instruments). In all experiments, *n* represents the number of different muscles used.

Ca^{2+} current measurements

Following earlier reports (Brigant and Mallart, 1982; Dudel, 1990; Slutsky et al., 2002; Kupchik et al., 2008), nerve action potential was evoked by superthreshold brief pulses (0.2 ms) given through a suction electrode. The excitatory nerve terminal current (ENTC) was measured by the macropatch electrode (Fig. 2 A). These experiments were performed in the presence of 50 nM TTX, which lowered both the amplitude of the axon action potential and that of the ENTC (Fig. 2 B). The ENTC consists of Ca^{2+}, leak, and capacitative currents. K^+ currents were blocked by 10 mM tetraethylammonium chloride and 100 µM 3,4-diaminopyridine added to the bath solution. Na^+ currents were blocked only under the electrode opening by adding 20 µM TTX inside the electrode. This enabled propagation of the action potential to the recording site. Then 100 µM Cd^{2+} was added to the bath to block the Ca^{2+} currents, and the remaining ENTC consisted of only leak and capacitative currents. This ENTC was then subtracted from the control ENTC (recorded without Cd^{2+}), yielding the net Ca^{2+} currents (Fig. 2 A). This procedure was repeated before and after uncaging of CNB-carbachol that produced 12 µM $[CCh^*]_{local}$ (for Fig. 2). The same procedure was used without and with Gal (for Fig. 3), and without and with three types of prepulses preceding the ENTC (for Figs. 5 and 7).

Establishing synaptic delay histograms

For establishing synaptic delay histograms (Katz and Miledi, 1965) the amplitude of the graded depolarizing pulse was lowered until mostly single quanta events were observed. To better resolve single quanta the temperature of the bathing solution was lowered to 10 ± 1°C. The low temperature slowed the release process and allowed detection of the earliest quanta events beyond the artifact. The delay between the beginning of the depolarizing pulse and the beginning of each quantum response was measured. Delay histograms were constructed by stacking the delays into 0.1-ms time bins and then connecting the midpoints of each time bin with a line. For comparison of the initial part of the histograms, each histogram was normalized to its peak and the initial part of the histograms was plotted on a faster time scale (Fig. 7).

Establishing the $DI_{release}$ curves

EPSCs were measured 1 s before (control) and 1 ms after the flash. Percentage of control release was first calculated for each pair of EPSCs (EPSC that followed the flash and its control), and then the results from all experiments were averaged. The data were fitted to Eq. 1, a variable-slope sigmoid DI curve:

$$Y = \frac{100}{1+10^{(\log IC_{50-release}-X)\times Hill}}, \quad (1)$$

where *Y* is the percentage of control release and *X* is the logarithm of concentration. $IC_{50\text{-}release}$ (the concentration for which 50% of control release is achieved) and *Hill* (the Hill coefficient which is taken from the sigmoid curve) were calculated by the computer program Prism (GraphPad Software; Slutsky et al., 2002). For all DI curves, $R^2 > 0.9$.

Calculating the "weighted concentration" of various drugs

In Fig. S3 F we show the "weighted" contribution of ACh, CCh, and Meth to the inhibition of release. The "weighted concentration" of each drug was determined by its ability to inhibit GCs using Eq. 2:

$$Weighted\_Concentration_{Drug} = [Drug]\times\frac{IC_{50-GCs}CCh}{IC_{50-GCs}Drug}. \quad (2)$$

Here, $Weighted\_Concentration_{Drug}$ denotes the weighted concentration of the drug applied. It is obtained by multiplying the actual drug concentration applied (*[Drug]*) by the ratio between the $IC_{50\text{-}GCs}$ of CCh ($IC_{50\text{-}GCs}CCh$) and of the drug ($IC_{50\text{-}GCs}Drug$). The effects of ACh and of CCh on the GCs were similar. Thus, for both drugs the weighted concentration equals the actual concentration applied. Because the $IC_{50\text{-}GCs}$ of Meth is ~5 times lower than that of CCh, its weighted concentration is ~5 times its actual concentration (i.e., 100 nM Meth is considered as ~500 nM).

The flash-photolysis experiments

The xenon lamp (Strobex 278; Chadwick-Helmuth) was mounted on the stereoscope binocular arm. The energy of the flash was 100 J; 20 s were required to recharge the lamp's capacitor. When measuring the effect of the flash on release, the beam of light (~7-mm diameter) was focused to the tip of the macropatch electrode and only then was CNB-carbachol added. As the light beam diameter was ~7 mm and the depth of the bathing solution above the muscle surface was <0.2 mm, the volume of the bathing solution that underwent uncaging was ≤0.03 ml. This ensured, in a 5-ml solution, a >150-fold dilution of the active CCh. Because we never applied more than five consecutive flashes, the overall concentration of CCh never accumulated to a steady-state level that affected release. This was also ensured by comparing the EPSCs measured before the first flash and seconds after the last flash. When measuring the effect of flash photolysis on GCs in oocytes, the light beam was focused on the oocyte. The solution was not circulated and only one flash was applied per oocyte.

Oocyte experiments

We used the same techniques as described previously (Ben-Chaim et al., 2003; Ohana et al., 2006). *Xenopus laevis* oocytes were isolated and incubated in NDE96 solution composed of ND96 (mM: 96 NaCl, 2 KCl, 1 $CaCl_2$, 1 $MgCl_2$, and 5 Hepes-NaOH, pH 7.5), 2.5 mM Na^+ pyruvate, 100 U/ml penicillin, and 100 µg/ml streptomycin (Dascal and Lotan, 1992). A day after their isolation, the oocytes were injected (Picospritzer, PLI-100; Medical Systems Corp.) with cRNAs. In vitro synthesis of RNA transcripts from the cloned cDNA was performed using standard procedures (Dascal and Lotan, 1992). The amounts of cRNA injected per oocyte were as follows: GIRK1 and GIRK2, 0.2 ng; $G\alpha_{i3}$, 1 ng; M_2R, 2 ng for GIRK current measurements; M_2R, 10 ng for GCs measurements. Currents were measured 3–5 d after cRNA injection.

Two-electrode voltage clamp

Currents were recorded using the standard two-electrode voltage clamp technique (Axoclamp 2B amplifier; Axon Instruments). The oocyte was impaled with two electrodes pulled from 1.5-mm borosilicate glass capillaries (Hilgenberg GmbH). Both electrodes were filled with 500 mM KCl solution. The recording and the current-passing electrode resistances were 15 and 1 MΩ, respectively. pCLAMP 8 software (Axon Instruments) was used for data acquisition and analysis.

Cut-open oocyte voltage clamp

GCs were measured as described previously (Stefani and Bezanilla, 1998; Ben-Chaim et al., 2006). The oocyte was impaled by a single electrode and recordings were performed at room temperature with a CA-1B amplifier (Dagan Corporation). Depolarizing pulses (from −120 mV to +40 mV for CCh, CNB-carbachol, and Meth; from −120 mV to −40 mV for Gal) were generated by using pCLAMP 8 software (Axon Instruments), a personal computer, and a DigiData 1322A interface (Axon Instruments). Data were sampled at 50 KHz and filtered at 5 kHz. The external solution contained (mM): 115 *N*-methyl-D-glucamine (NMDG)-methanesulphonate, 2 $CaCl_2$, and 20 Hepes. pH was adjusted to 7.5. The internal solution was similar but without $CaCl_2$, and contained 2 mM EGTA. CCh, Gal, Meth, or CNB-carbachol was added by first diluting them in external solution and then replacing the regular external solution (control) with this modified solution. In each oocyte, GCs were measured under control conditions and then after addition of one concentration of the tested drug (excluding Fig. 1 B, where GCs under all $[CCh]_o$ were measured in the same oocyte). Data were used only when the total charge (integral of the total current) of the On and Off responses was similar. Although with CCh this was the case when depolarizing the oocyte to +40 mV, Gal affected the On response voltage-dependently at depolarizations higher than −40 mV. This could mean that at high depolarizations the On currents are contaminated by currents from other sources. Thus, for the Gal experiments the oocyte was depolarized from −120 mV to −40 mV. The percentage of inhibition was obtained by the ratio between the total charge with the drug and the total charge without the drug. Then all results were normalized to their controls, and data were averaged. For the DI curves, results were fitted with Eq. 1 (for GCs, *Y* is the percentage of control GCs, and $IC_{50\text{-}release}$ was replaced by $IC_{50\text{-}GCs}$. All other parameters are the same). To subtract the linear portion of capacitative current from the records we used the pulse/8 procedure described previously (Bezanilla and Armstrong, 1977; Ben-Chaim et al., 2006).

The current from eight "subtraction" pulses of amplitude of one eighth (20 mV) of the depolarizing pulse (160 mV) was digitally subtracted from the current produced by the depolarizing pulse. The reason why the pulse/8 procedure gives 8 pulses is because the current produced by a single pulse of one eighth of the depolarizing pulse amplitude would have to be multiplied by eight before it could be subtracted from the current produced by the depolarizing pulse. One should design the direction of the subtraction pulses so that they occur in the region where no gating charge moves. Therefore, subtraction pulses were applied from a holding potential of +30 mV, where no charge movement was observed. This procedure was repeated 10 times to improve signal-to-noise ratio.

M_2R-induced GIRK currents

The M_2R-induced GIRK currents served to calibrate $[CCh^*]_{local}$ produced by the flash in the release experiments and to examine whether Gal induces production of $G_{\beta\gamma}$. To measure the M_2R-induced GIRK currents, oocytes injected with cRNA of GIRK1, GIRK2, $G\alpha_{i3}$, and M_2R were voltage clamped at −80 mV in ND96 solution. cRNA of $G\alpha_{i3}$ was injected in order to decrease the basal GIRK current (I_K) that is produced by free endogenous $G_{\beta\gamma}$ (Dascal, 1997) and thus to improve the relative activation of the GIRK channels by the agonist (Peleg et al., 2002). To measure K^+ currents, ND96 was replaced by 24 mM K^+ solution (similar to ND96 but with 72 mM NaCl, 24 mM KCl, and pH adjusted with KOH), and I_K appeared. Subsequent addition of 5 µM Gal did not increase I_K. For calibrating $[CCh^*]_{local}$, $[CCh]_o$ was elevated stepwise to produce the DR curve, without washout between steps, and the corresponding GIRK currents (I_{CCh}) were measured for the various $[CCh]_o$. I_{CCh} was terminated upon CCh washout. For calibration of $[CCh^*]_{local}$ a 50-µl drop of 10 mM CNB-carbachol was positioned under the flash lamp, so that the entire drop would undergo flash-photolysis. After the flash was administered, the entire drop was transferred to 50 ml (1,000x dilution) 24 mM K^+ solution and this new solution was applied to the oocyte and produced I_{CCh^*}. The concentration of CCh* (the active portion of CCh created after the flash) could be calculated using I_{CCh^*}. Thus, we could estimate the efficiency of the flash (percent uncaging) throughout the flash experiments (Fig. S2) and hence $[CCh^*]_{local}$ at the various $[CNB\text{-}carbachol]_o$.

The DR curves were fitted with Eq. 3, a Michaelis-Menten type equation assuming two agonist binding sites (Ben-Chaim et al., 2003),

$$Y = \frac{B_{\max} \times X^2}{\left(K_d + X\right)^2} \quad (3)$$

where Y is the fractional amplitude of the current at any agonist concentration, B_{max} is the response to saturating concentration of agonist defined as 100%, X is the concentration of the agonist (CCh), and K_d denotes the dissociation constant.

Materials

Penicillin-streptomycin was purchased from Biological Industries. D(+)-glucose was purchased from Riedel-de Haën. Saponin, *N*-methyl-D-glucamine (NMDG)-methanesulphonate, EGTA, Hepes, pyruvate, ACh, Meth, Gal, and CCh were purchased from Sigma-Aldrich. Tetrodotoxin (TTX) was purchased from Alomone Laboratories. CNB-carbachol was purchased from Invitrogen.

Statistical analyses

Significance of effects was verified throughout the paper (except in Fig. 7) using the student's unpaired *t* test. In Fig. 7 significance was measured with the Kolmogorov-Smirnov test. Error bars in figures represent SEM. All statistical analyses were performed using Prism version 4.03 for Windows (GraphPad Software).

Online supplemental material

Fig. S1 shows inhibition of GCs by ACh. Fig. S2 shows the calibration of the amount of CNB-carbachol uncaged after a flash. Fig. S3 shows the effect of Meth on M_2R GCs and on release in various conditions. Fig. S4 shows the combined effect of the GCs and of Ca^{2+} on the amount of release. Video 1 shows our suggested mechanism for control of neurotransmitter release. Online supplemental material is available at http://www.jcb.org/cgi/content/full/jcb.201007053/DC1.

We thank Professor Micha Spira for his insightful suggestions and comments. We are grateful to Dr. Kenneth Stein and the Goldie-Anna fund for their support.

Submitted: 12 July 2010
Accepted: 3 December 2010

References

Andreu, R., and E.F. Barrett. 1980. Calcium dependence of evoked transmitter release at very low quantal contents at the frog neuromuscular junction. *J. Physiol.* 308:79–97.

Ben-Chaim, Y., O. Tour, N. Dascal, I. Parnas, and H. Parnas. 2003. The M2 muscarinic G-protein-coupled receptor is voltage-sensitive. *J. Biol. Chem.* 278:22482–22491. doi:10.1074/jbc.M301146200

Ben-Chaim, Y., B. Chanda, N. Dascal, F. Bezanilla, I. Parnas, and H. Parnas. 2006. Movement of 'gating charge' is coupled to ligand binding in a G-protein-coupled receptor. *Nature.* 444:106–109. doi:10.1038/nature05259

Bezanilla, F., and C.M. Armstrong. 1977. Inactivation of the sodium channel. I. Sodium current experiments. *J. Gen. Physiol.* 70:549–566. doi:10.1085/jgp.70.5.549

Blackmer, T., E.C. Larsen, C. Bartleson, J.A. Kowalchyk, E.J. Yoon, A.M. Preininger, S. Alford, H.E. Hamm, and T.F. Martin. 2005. G protein betagamma directly regulates SNARE protein fusion machinery for secretory granule exocytosis. *Nat. Neurosci.* 8:421–425.

Bollmann, J.H., and B. Sakmann. 2005. Control of synaptic strength and timing by the release-site Ca2+ signal. *Nat. Neurosci.* 8:426–434.

Bollmann, J.H., B. Sakmann, and J.G. Borst. 2000. Calcium sensitivity of glutamate release in a calyx-type terminal. *Science.* 289:953–957. doi:10.1126/science.289.5481.953

Brigant, J.L., and A. Mallart. 1982. Presynaptic currents in mouse motor endings. *J. Physiol.* 333:619–636.

Calakos, N., and R.H. Scheller. 1996. Synaptic vesicle biogenesis, docking, and fusion: a molecular description. *Physiol. Rev.* 76:1–29.

Conn, P.J., A. Christopoulos, and C.W. Lindsley. 2009. Allosteric modulators of GPCRs: a novel approach for the treatment of CNS disorders. *Nat. Rev. Drug Discov.* 8:41–54. doi:10.1038/nrd2760

Daeffler, L., A. Chahdi, J.P. Gies, and Y. Landry. 1999. Inhibition of GTPase activity of Gi proteins and decreased agonist affinity at M2 muscarinic acetylcholine receptors by spermine and methoctramine. *Br. J. Pharmacol.* 127:1021–1029. doi:10.1038/sj.bjp.0702625

Dascal, N. 1997. Signalling via the G protein-activated K+ channels. *Cell. Signal.* 9:551–573. doi:10.1016/S0898-6568(97)00095-8

Dascal, N., and I. Lotan. 1992. Expression of exogenous ion channels and neurotransmitter receptors in RNA-injected *Xenopus* oocytes. *In* Methods in Molecular Neurobiology. A. Longstaff and P. Revest, editors. Humana Press, Totowa, NJ. 205–225.

Datyner, N.B., and P.W. Gage. 1980. Phasic secretion of acetylcholine at a mammalian neuromuscular junction. *J. Physiol.* 303:299–314.

Del Castillo, J., and B. Katz. 1954. The effect of magnesium on the activity of motor nerve endings. *J. Physiol.* 124:553–559.

Dodge, F.A. Jr., and R. Rahamimoff. 1967. Co-operative action a calcium ions in transmitter release at the neuromuscular junction. *J. Physiol.* 193:419–432.

Dolphin, A.C. 1998. Mechanisms of modulation of voltage-dependent calcium channels by G proteins. *J. Physiol.* 506:3–11. doi:10.1111/j.1469-7793.1998.003bx.x

Dudel, J. 1981. The effect of reduced calcium on quantal unit current and release at the crayfish neuromuscular junction. *Pflugers Arch.* 391:35–40. doi:10.1007/BF00580691

Dudel, J. 1990. Inhibition of Ca2+ inflow at nerve terminals of frog muscle blocks facilitation while phasic transmitter release is still considerable. *Pflugers Arch.* 415:566–574. doi:10.1007/BF02583507

Felmy, F., E. Neher, and R. Schneggenburger. 2003a. Probing the intracellular calcium sensitivity of transmitter release during synaptic facilitation. *Neuron.* 37:801–811. doi:10.1016/S0896-6273(03)00085-0

Felmy, F., E. Neher, and R. Schneggenburger. 2003b. The timing of phasic transmitter release is Ca2+-dependent and lacks a direct influence of presynaptic membrane potential. *Proc. Natl. Acad. Sci. USA.* 100:15200–15205. doi:10.1073/pnas.2433276100

Gether, U. 2000. Uncovering molecular mechanisms involved in activation of G protein-coupled receptors. *Endocr. Rev.* 21:90–113. doi:10.1210/er.21.1.90

Gomeza, J., H. Shannon, E. Kostenis, C. Felder, L. Zhang, J. Brodkin, A. Grinberg, H. Sheng, and J. Wess. 1999. Pronounced pharmacologic deficits in M2 muscarinic acetylcholine receptor knockout mice. *Proc. Natl. Acad. Sci. USA.* 96:1692–1697. doi:10.1073/pnas.96.4.1692

Gregory, K.J., P.M. Sexton, and A. Christopoulos. 2007. Allosteric modulation of muscarinic acetylcholine receptors. *Curr. Neuropharmacol.* 5:157–167. doi:10.2174/157015907781695946

Hamm, H.E. 1998. The many faces of G protein signaling. *J. Biol. Chem.* 273:669–672. doi:10.1074/jbc.273.2.669

Hochner, B., H. Parnas, and I. Parnas. 1991. Effects of intra-axonal injection of Ca2+ buffers on evoked release and on facilitation in the crayfish neuromuscular junction. *Neurosci. Lett.* 125:215–218. doi:10.1016/0304-3940(91)90032-O

Ilouz, N., L. Branski, J. Parnis, H. Parnas, and M. Linial. 1999. Depolarization affects the binding properties of muscarinic acetylcholine receptors and their interaction with proteins of the exocytic apparatus. *J. Biol. Chem.* 274:29519–29528. doi:10.1074/jbc.274.41.29519

Jakubík, J., L. Bacáková, V. Lisá, E.E. el-Fakahany, and S. Tucek. 1996. Activation of muscarinic acetylcholine receptors via their allosteric binding sites. *Proc. Natl. Acad. Sci. USA.* 93:8705–8709. doi:10.1073/pnas.93.16.8705

Katz, B., and R. Miledi. 1965. The measurement of synaptic delay, and the time course of acetylcholine release at the neuromuscular junction. *Proc. R. Soc. Lond., B, Biol. Sci.* 161:483–495. doi:10.1098/rspb.1965.0016

Katz, B., and R. Miledi. 1978. A re-examination of curare action at the motor endplate. *Proc. R. Soc. Lond., B, Biol. Sci.* 203:119–133. doi:10.1098/rspb.1978.0096

Kew, J.N.C., J.M. Ducarre, M.C. Pflimlin, V. Mutel, and J.A. Kemp. 2001. Activity-dependent presynaptic autoinhibition by group II metabotropic glutamate receptors at the perforant path inputs to the dentate gyrus and CA1. *Neuropharmacology.* 40:20–27. doi:10.1016/S0028-3908(00)00118-0

Khanin, R., H. Parnas, and L. Segel. 1997. "First step" negative feedback accounts for inhibition of fast neurotransmitter release. *J. Theor. Biol.* 188:261–276. doi:10.1006/jtbi.1997.0480

Kupchik, Y.M., G. Rashkovan, L. Ohana, T. Keren-Raifman, N. Dascal, H. Parnas, and I. Parnas. 2008. Molecular mechanisms that control initiation and termination of physiological depolarization-evoked transmitter release. *Proc. Natl. Acad. Sci. USA.* 105:4435–4440. doi:10.1073/pnas.0708540105

Lee, N.H., and E.E. el-Fakahany. 1991. Allosteric antagonists of the muscarinic acetylcholine receptor. *Biochem. Pharmacol.* 42:199–205. doi:10.1016/0006-2952(91)90703-8

Linial, M., N. Ilouz, and H. Parnas. 1997. Voltage-dependent interaction between the muscarinic ACh receptor and proteins of the exocytic machinery. *J. Physiol.* 504:251–258. doi:10.1111/j.1469-7793.1997.251be.x

Llinás, R., I.Z. Steinberg, and K. Walton. 1981. Presynaptic calcium currents in squid giant synapse. *Biophys. J.* 33:289–321. doi:10.1016/S0006-3495(81)84898-9

Loiacono, R., J. Stephenson, J. Stevenson, and F. Mitchelson. 1993. Multiple binding sites for nicotine receptor antagonists in inhibiting [3H](-)-nicotine binding in rat cortex. *Neuropharmacology.* 32:847–853. doi:10.1016/0028-3908(93)90139-T

Lustig, C., H. Parnas, and L.A. Segel. 1989. Neurotransmitter release: development of a theory for total release based on kinetics. *J. Theor. Biol.* 136:151–170. doi:10.1016/S0022-5193(89)80222-X

Martin, A.R. 1966. Quantal nature of synaptic transmission. *Physiol. Rev.* 46:51.

Milburn, T., N. Matsubara, A.P. Billington, J.B. Udgaonkar, J.W. Walker, B.K. Carpenter, W.W. Webb, J. Marque, W. Denk, J.A. McCray, et al. 1989. Synthesis, photochemistry, and biological activity of a caged photolabile acetylcholine receptor ligand. *Biochemistry.* 28:49–55. doi:10.1021/bi00427a008

Mitchelson, F. 1988. Muscarinic receptor differentiation. *Pharmacol. Ther.* 37:357–423. doi:10.1016/0163-7258(88)90005-8

Murthy, V.N., and P. De Camilli. 2003. Cell biology of the presynaptic terminal. *Annu. Rev. Neurosci.* 26:701–728. doi:10.1146/annurev.neuro.26.041002.131445

Neher, E., and T. Sakaba. 2008. Multiple roles of calcium ions in the regulation of neurotransmitter release. *Neuron.* 59:861–872. doi:10.1016/j.neuron.2008.08.019

Ohana, L., O. Barchad, I. Parnas, and H. Parnas. 2006. The metabotropic glutamate G-protein-coupled receptors mGluR3 and mGluR1a are voltage-sensitive. *J. Biol. Chem.* 281:24204–24215. doi:10.1074/jbc.M513447200

Pan, B., and R.S. Zucker. 2009. A general model of synaptic transmission and short-term plasticity. *Neuron.* 62:539–554. doi:10.1016/j.neuron.2009.03.025

Parnas, H., and I. Parnas. 2007. The chemical synapse goes electric: Ca2+- and voltage-sensitive GPCRs control neurotransmitter release. *Trends Neurosci.* 30:54–61. doi:10.1016/j.tins.2006.12.001

Parnas, I., and H. Parnas. 2010. Control of neurotransmitter release: From Ca2+ to voltage dependent G-protein coupled receptors. *Pflugers Arch.* 460:975–990. doi:10.1007/s00424-010-0872-7

Parnas, H., L. Segel, J. Dudel, and I. Parnas. 2000. Autoreceptors, membrane potential and the regulation of transmitter release. *Trends Neurosci.* 23:60–68. doi:10.1016/S0166-2236(99)01498-8

Parnas, H., J.C. Valle-Lisboa, and L.A. Segel. 2002. Can the Ca2+ hypothesis and the Ca2+-voltage hypothesis for neurotransmitter release be reconciled? *Proc. Natl. Acad. Sci. USA.* 99:17149–17154. doi:10.1073/pnas.242549999

Parnas, H., I. Slutsky, G. Rashkovan, I. Silman, J. Wess, and I. Parnas. 2005. Depolarization initiates phasic acetylcholine release by relief of a tonic block imposed by presynaptic M2 muscarinic receptors. *J. Neurophysiol.* 93:3257–3269. doi:10.1152/jn.01131.2004

Peleg, S., D. Varon, T. Ivanina, C.W. Dessauer, and N. Dascal. 2002. G(alpha)(i) controls the gating of the G protein-activated K(+) channel, GIRK. *Neuron.* 33:87–99. doi:10.1016/S0896-6273(01)00567-0

Schneggenburger, R., and E. Neher. 2000. Intracellular calcium dependence of transmitter release rates at a fast central synapse. *Nature.* 406:889–893. doi:10.1038/35022702

Schneggenburger, R., and E. Neher. 2005. Presynaptic calcium and control of vesicle fusion. *Curr. Opin. Neurobiol.* 15:266–274. doi:10.1016/j.conb.2005.05.006

Slutsky, I., H. Parnas, and I. Parnas. 1999. Presynaptic effects of muscarine on ACh release at the frog neuromuscular junction. *J. Physiol.* 514:769–782. doi:10.1111/j.1469-7793.1999.769ad.x

Slutsky, I., I. Silman, I. Parnas, and H. Parnas. 2001. Presynaptic M(2) muscarinic receptors are involved in controlling the kinetics of ACh release at the frog neuromuscular junction. *J. Physiol.* 536:717–725. doi:10.1111/j.1469-7793.2001.00717.x

Slutsky, I., G. Rashkovan, H. Parnas, and I. Parnas. 2002. Ca2+-independent feedback inhibition of acetylcholine release in frog neuromuscular junction. *J. Neurosci.* 22:3426–3433.

Slutsky, I., J. Wess, J. Gomeza, J. Dudel, I. Parnas, and H. Parnas. 2003. Use of knockout mice reveals involvement of M2-muscarinic receptors in control of the kinetics of acetylcholine release. *J. Neurophysiol.* 89:1954–1967. doi:10.1152/jn.00668.2002

Stefani, E., and F. Bezanilla. 1998. Cut-open oocyte voltage-clamp technique. *Methods Enzymol.* 293:300–318. doi:10.1016/S0076-6879(98)93020-8

Sudhof, T.C. 2004. The synaptic vesicle cycle. *Annu. Rev. Neurosci.* 27:509–547. doi:10.1146/annurev.neuro.26.041002.131412

Wonnacott, S. 1997. Presynaptic nicotinic ACh receptors. *Trends Neurosci.* 20:92–98. doi:10.1016/S0166-2236(96)10073-4

Yusim, K., H. Parnas, and L. Segel. 1999. Theory of fast neurotransmitter release control based on voltage-dependent interaction between autoreceptors and proteins of the exocytotic machinery. *Bull. Math. Biol.* 61:701–725. doi:10.1006/bulm.1999.0107

Zohar, A., N. Dekel, B. Rubinsky, and H. Parnas. 2010. New mechanism for voltage induced charge movement revealed in GPCRs—theory and experiments. *PLoS One.* 5:e8752. doi:10.1371/journal.pone.0008752